Journal of Power Sources 247 (2014) 437–443

Contents lists available at ScienceDirect

Journal of Power Sources

journal homepage: www.elsevier.com/locate/jpowsour

Two-step oxalate approach for the preparation of high performance $LiNi_{0.5}Mn_{1.5}O_4$ cathode material with high voltage

Zushan Liu, Yangmei Jiang, Xiaoyuan Zeng, Guan Xiao, Huiyu Song, Shijun Liao*

The Key Laboratory of Fuel Cell Technology of Guangdong Province & The Key Laboratory of New Energy Technology of Guangdong Universities, School of Chemistry and Chemical Engineering, South China University of Technology, Guangzhou 510641, China

HIGHLIGHTS

- Spinel $LiNi_{0.5}Mn_{1.5}O_4$ materials are synthesized by a two-step approach.
- The spinel oxide precursor is derived from the oxalate precipitation.
- The materials had capacities of 136 mAh g^{-1} at C/10 rate and good cycle stability.
- The calcining temperature plays an important role for the performance of the materials.

ARTICLE INFO

Article history:
Received 17 July 2013
Received in revised form
31 August 2013
Accepted 1 September 2013
Available online 11 September 2013

Keywords:
Two-step approach
Lithium nickel manganate
Cathode
Lithium ion battery

ABSTRACT

A high voltage cathode material, $LiNi_{0.5}Mn_{1.5}O_4$, is synthesized with a two-step approach, in which the nickel–manganese oxalate precipitate is firstly obtained by adding oxalic acid to the solution of nickel and manganese ions precursors, followed by calcining the oxalates to obtain spinel nickel–manganese oxide, incorporating lithium ions with ball milling and calcining at 900 °C for 15 h. The materials are characterized with TG, XRD, SEM, BET and FTIR; it is revealed that both nickel–manganese oxide and final $LiNi_{0.5}Mn_{1.5}O_4$ have well defined spinel structure. The $LiNi_{0.5}Mn_{1.5}O_4$ spinel materials exhibit high capacities and good cyclic stability, the capacity of the materials is in the range from 126 to 136 mAh $^{-1}$, depending on the calcining temperatures. The sample calcined at an optimal temperature of 900 °C exhibits best performance, the capacity is high up to 136 mAh g^{-1} at tenth cycle and the capacity retention after 50 cycles is 93%. For the sample prepared by mixing and milling oxalate with lithium salt, the discharge capacity is only 115 mAh g^{-1}. We suggest that the spinel oxide derived from oxalate may play an important role for the high performance and high stability of the final cathode materials.

1. Introduction

Spinel lithium manganate ($LiMn_2O_4$) has gained tremendous attention due to its low cost, environmental friendliness and high safety [1,2]. However, stoichiometric $LiMn_2O_4$ is a problematic cathode material because of its significant capacity fade, which needs further improvements [3,4]. In order to overcome the vital problem of this promising material, various 3d-transition metal ions are substituted for Mn to form binary $LiM_xMn_{2-x}O_4$ (M = Co, Cr, Cu, Fe, Ni) materials [5], which show a high voltage plateau at 4.7–5.1 V. Among them, Ni-substituted material $LiNi_{0.5}Mn_{1.5}O_4$ is of great interest as a cathode material because of its superior energy density and high voltage plateau at around 4.7 V, which arise from the presence of a Ni^{4+}/Ni^{2+} redox pair [6,7].

Various methods such as solid state reaction [8–10], co-precipitation [11–16], spray drying process [17] and sol–gel [18,19] have been developed for the preparation of $LiNi_{0.5}Mn_{1.5}O_4$ materials. The solid state reaction is generally recognized as a simple and low cost process to prepare $LiNi_{0.5}Mn_{1.5}O_4$ materials. Nevertheless, this method has some disadvantages such as inhomogeneity, uncontrollable particle growth and agglomeration, thus, the materials prepared with solid state method usually exhibit unsatisfied performance.

Preparing $LiNi_{0.5}Mn_{1.5}O_4$ materials through co-precipitation method has been investigated by some researchers recently [20–22]. Generally the potassium hydroxide (KOH) or sodium hydroxide (NaOH) were used as precipitator, the materials were prepared by obtaining hydroxide precursor $Mn_{0.75}Ni_{0.25}(OH)_2$ firstly, followed by washing and filtering to remove potassium or sodium

* Corresponding author. Fax: +86 20 87113586.
E-mail address: chsjliao@scut.edu.cn (S. Liao).

0378-7753/$ – see front matter © 2013 Elsevier B.V. All rights reserved.
http://dx.doi.org/10.1016/j.jpowsour.2013.09.002

ions, mixing with lithium hydrate or lithium carbonate, and calcining at various temperatures. The most important advantage of co-precipitation procedure is easy to realize homogeneous mixing.

Although the binary spinel oxide have already been reported previously to be used as intermediate for the preparation of $LiNi_{0.5}Mn_{1.5}O_4$ [23], and a few of works adopted the oxalate co-precipitation approach also has been reported [24]. However, there are no literature reported the two-step oxalate route as described below.

In this work, we attempted to synthesize spinel $LiNi_{0.5}Mn_{1.5}O_4$ cathode materials with a new two-step approach, in which the spinel oxide precursor was derived from the co-precipitate of Ni and Mn oxalates, instead of the hydroxides or carbonate. We adopted oxalate route based on following consideration. Firstly, oxalic acid is a cheap organic material, and a rather mild precipitant compared with the hydroxide or carbonate, which is beneficial to get the homogeneous precipitate. Secondly, the oxide derived from the decomposition of organic precursors is generally superior to that derived from the decomposition of hydroxide or carbonate precursors, such as higher surface area, better porous structure, smaller particle size, etc. As we expected, due to our binary oxide is derived from the decomposition of oxalate, the final $LiNi_{0.5}Mn_{1.5}O_4$ materials exhibited high capacity and good stability.

2. Experimental

2.1. Preparation of $LiNi_{0.5}Mn_{1.5}O_4$ materials

Manganese acetate tetrahydrate ($Mn(CH_3COO)_2{\cdot}4H_2O$, 99.0%, Kermel) was used as Mn source, nickel acetate tetrahydrate ($Ni(CH_3COO)_2{\cdot}4H_2O$, 98.0%, Kermel) as Ni source, lithium carbonate (Li_2CO_3, 97.0%, Kermel) as Li source, and the oxalic acid dihydrate ($C_2H_2O_4{\cdot}2H_2O$, 99.5%, Enox) was used as precipitant.

$LiNi_{0.5}Mn_{1.5}O_4$ materials were prepared by the following two-step procedure. In the first step, a binary oxalate co-precipitate was firstly prepared by adding oxalic acid solution to the solution containing manganese acetate tetrahydrate and nickel acetate tetrahydrate, followed by stirring and drying overnight. Then spinel structured manganese–nickel (Mn–Ni) binary oxide was prepared by calcining the oxalate at 550 °C for 5 h. In the second step, $LiNi_{0.5}Mn_{1.5}O_4$ materials were prepared by mixing and ball milling the mixture of the binary oxide and lithium carbonate, followed by calcining at 750–950 °C in air for 15 h with a heating rate of 5 K min^{-1} and a cooling rate of 2 K min^{-1}.

For the purpose of comparison, we also prepared a $LiNi_{0.5}Mn_{1.5}O_4$ sample followed the above route, finally calcined at 900 °C, but mixing and milling Mn–Ni oxalate with lithium carbonate directly, instead of mixing and milling Mn–Ni oxide with lithium carbonate. We denoted this sample as LNMO-OX.

2.2. Physical characterization

The crystal structure of samples was identified by X-ray diffraction (XRD, TD-3500, Tongda, China) using Cu $K_{\alpha 1}$ radiation operated at 30 kV and 20 mA with a scan rate of 4° min^{-1} from 10° to 70°. The particle morphologies were observed using scanning electron microscope (SEM, JSM-6380, JEOL/EO, Japan). The N_2 adsorption–desorption isotherms were measured with Tristar ASAP 3020 gas adsorption analyzer, and the specific surface area was calculated by the Brunauer–Emmett–Teller (BET) method. A Fourier transform infrared spectrometer (Tensor 27, Bruker, Germany) was used for the IR analysis, and the sample preparation for FTIR was carried out by diluting a small amount of powders in 100 mg of KBr powders. The thermal gravimetric analysis was performed with a thermal analyzer (TG, Q600 SDT, TAINC, America).

2.3. Electrochemical testing

Electrochemical evaluation of materials was performed with CR-2016 coin cells using lithium metal as the negative electrode. The positive electrode was prepared by mixing $LiNi_{0.5}Mn_{1.5}O_4$ material, acetylene black, and polyvinylidene fluoride (PVDF) binder with mass proportion of 78:12:10 in N-methyl-2-pyrrolidone (NMP) to form slurry. Then the slurry was coated onto an aluminum foil, which served as a current collector, followed by drying at 110 °C for 12 h in a vacuum oven. Finally, the cathode material-coated foils were pressed under 15 MPa for 3 min, with a final material loading about 7–10 mg cm^{-2}. The cells were fabricated in a vacuum glove box filled with argon, with lithium plate as the negative electrode, Celgard 2400 single polypropylene layer separator as the separator (Celgard 2400, Celgard, America), and 1 M lithium hexafluorophosphate ($LiPF_6$) solution, in which a mixture of ethylene carbonate (EC) and dimethyl carbonate (DMC) (1:1 in volume) was used as the solvent, as the electrolyte.

The prepared cells were tested on a battery testing system (Neware, CT-3008, China) with various charge–discharge rates at room temperature. The voltage range for the charge–discharge is between 3.5 and 4.9 V (vs. Li^+/Li).

3. Results and discussion

3.1. Structure characterization

To reveal the conversion process from nickel manganese oxalate to the spinel oxide, we analyzed the sample with thermal analysis technique. Fig. 1 shows the thermal analysis curves (TG/DTA) of the nickel manganese oxalate. The weight losses and endothermic peaks at 60 °C and 113 °C can be interpreted as the release of residual adsorbed water, and the 13.5% weight loss began at 130 °C, with an endothermic peak at 194 °C, might be the removal of crystalliferous water incorporated in the lattice of the material. At 292 °C, the weight loss is high up to 34.5%, accompanied with a very strong exothermal peak, it may result from the conversion of oxalate anion into CO_2 and H_2O, as well as nickel manganese oxalate into the binary oxide.

Fig. 2a shows the XRD patterns of the oxalate precursors calcined at 450 and 550 °C. It is clearly that, a crystallite did not well

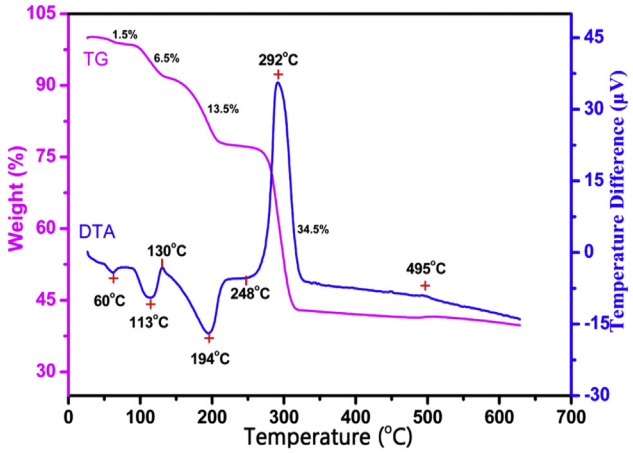

Fig. 1. Thermal gravimetry of the nickel manganese oxalate precursors, heating rate: 5 K min^{-1}.

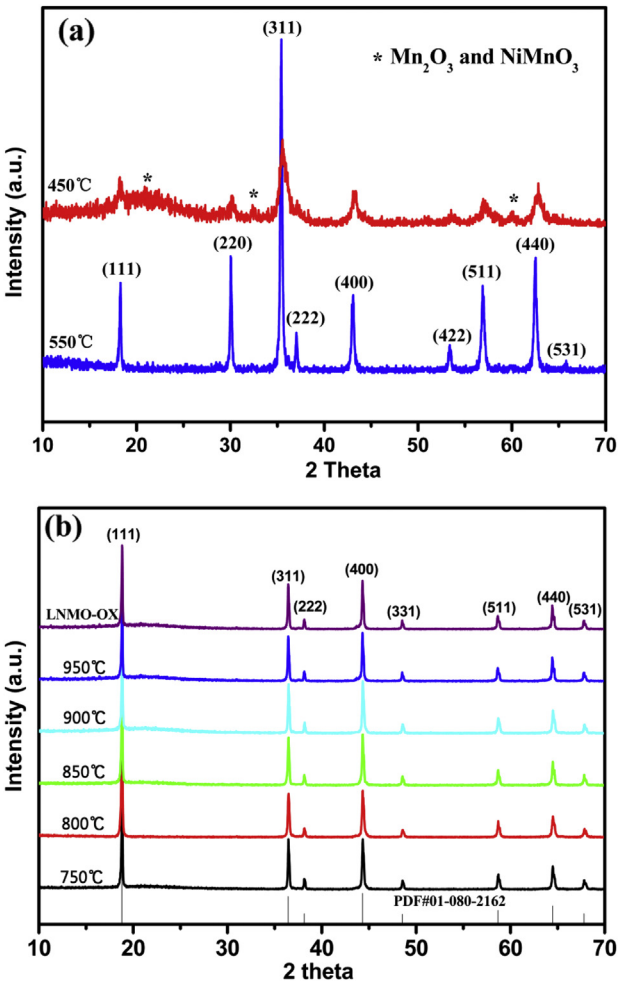

Fig. 2. The XRD patterns of the oxides precursor derived from oxalate by calcining at 450 and 550 °C for 5 h (a) and the final $LiNi_{0.5}Mn_{1.5}O_4$ cathode materials prepared at different calcining temperatures (b).

formed when the samples were calcined at 450 °C, and a few of nickel and manganese oxide can be observed. However, a pure $Ni_{0.67}Mn_2O_4$ spinel phase was obtained when the oxalate precursors were calcined at 550 °C, which is in good agreement with $Ni_{1-x}Mn_2O_4$ ($x = 0.33$) reported by Hagh et al. [10].

Fig. 2b shows the XRD patterns of $LiNi_{0.5}Mn_{1.5}O_4$ cathode materials, the peaks of the six samples agreed well with the spinel phase $LiNi_{0.5}Mn_{1.5}O_4$ in the standard Powder Diffraction Card (no. 01-080-2162). It should be pointed out that the XRD pattern of the sample LNMO-OX, which is prepared by mixing and milling oxalate with lithium carbonate, is almost same to that of sample prepared via spinel Mn–Ni binary oxide. However, as shown in Fig. 6a, the material prepared via spinel Mn–Ni binary oxide route exhibits much better capacity than the material prepared by mixing and milling oxalate with lithium carbonate directly.

Metal ion ordering in octahedral sites of the $LiNi_{0.5}Mn_{1.5}O_4$ structure results in the assignment to either a space group of $P4_332$ or Fd-3m [25,26]. The former represents the Mn and Ni ions ordering in the 12d and 4b sites, while the latter indicates the random occupation of Ni and Mn ions in the 16d site of octahedral. In most cases, synthesized samples both contained these two space group structures. However, identification of these two groups by X-ray diffraction is difficult to achieve because of a very weak diffraction peaks of super-lattice lines of (1 1 0), (2 1 0), (3 1 0) in the

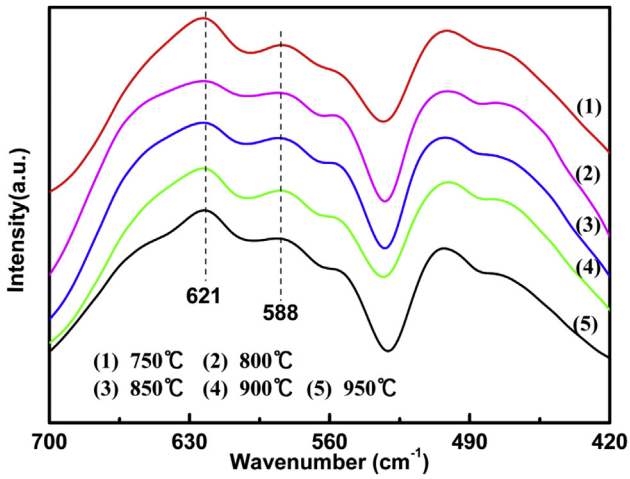

Fig. 3. FTIR spectra of spinel $LiNi_{0.5}Mn_{1.5}O_4$ calcined at different temperatures.

ordered spinel structure. Generally, FTIR is an efficient technique which can easily determine the cation ordering [27].

The cation ordering in $LiNi_{0.5}Mn_{1.5}O_4$ spinel materials could be characterized by a comparison of the FTIR intensity ratio between the 588 cm^{-1} Ni–O band and the 621 cm^{-1} Mn–O band, which is considered to be a semi-quantitative measure of the fraction of cation ordering in the sample [28,29]. Fig. 3 illustrates the FTIR curves of the $LiNi_{0.5}Mn_{1.5}O_4$ powders calcined in the temperature range of 750–950 °C. Table 1 gives the specific FTIR data of the absorption intensity at 588 cm^{-1} and 621 cm^{-1}. As we can see in Fig. 3 and Table 1, all the samples are confirmed with a main space group of Fd-3m with a small part of $P4_332$. The sample annealed at 800 °C exhibits the highest intensity ratio of the 588 cm^{-1} peak to the 621 cm^{-1} peak in the FTIR spectra compared to other four samples, indicating a relatively higher degree of ordering of the Mn and Ni ions in this sample. When temperature is higher than 800 °C, the intensity ratio decreases with the increasing of calcining temperatures, indicating the ratio of disordered structure increases, namely the amount of Mn^{3+} in the materials increases, which was the same as reported before [20]. Since the integrated crystallite is not very well formed when the calcining temperature is at 750 °C, so the ratio of disordered structure is relatively higher than 800 °C.

3.2. Morphology characterization

Fig. 4 shows the SEM images of the oxide precursors and the $LiNi_{0.5}Mn_{1.5}O_4$ materials prepared at different calcining temperatures. Fig. 4a and b shows the spinel oxide precursors calcined at 450 and 550 °C. It is clearly that only cloud-like and not well crystallized amorphous materials can be observed for the oxide

Table 1
FTIR absorption intensity and ratio of I_{588}/I_{621} of samples calcined at different temperatures.

Calcining temperature (°C)	Absorption intensity I (621 cm^{-1})	Absorption intensity I (588 cm^{-1})	Intensity ratio I (588 cm^{-1})/ I (621 cm^{-1})
750	0.24686	0.36069	1.4611
800	0.05263	0.10068	1.9130
850	0.09379	0.15655	1.6692
900	0.21152	0.30319	1.4334
950	0.31136	0.42647	1.3697

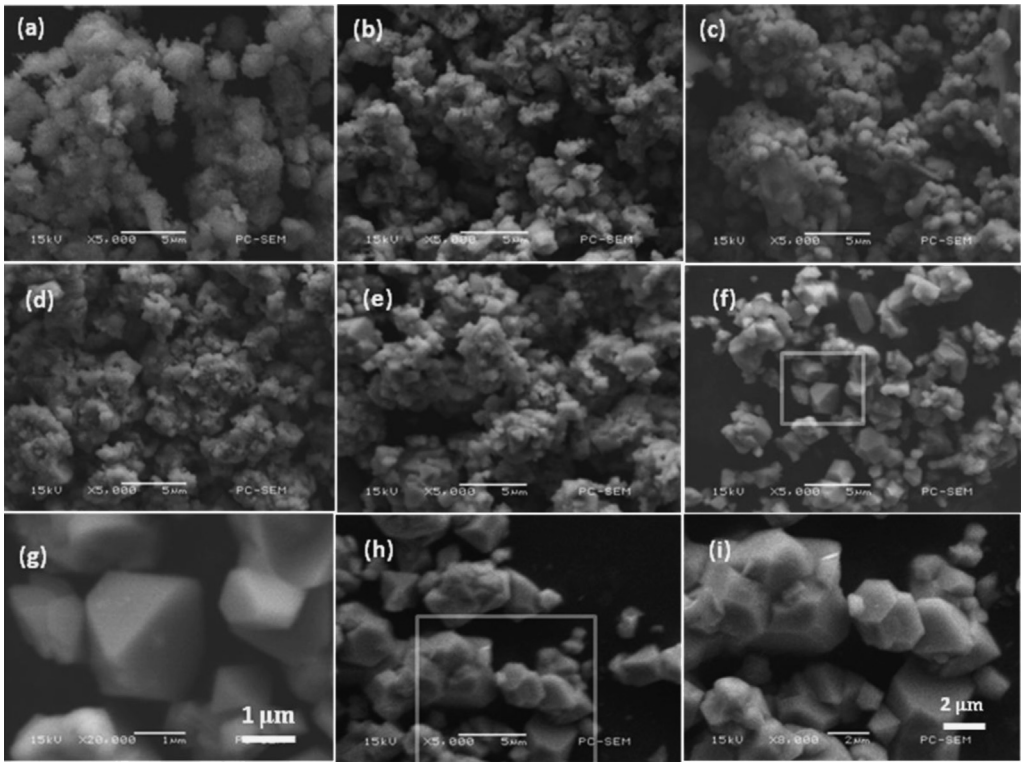

Fig. 4. SEM images of the oxide precursors derived from oxalates calcined at 450 °C (a) and 550 °C (b) for 5 h, and the $LiNi_{0.5}Mn_{1.5}O_4$ materials prepared at different calcining temperatures, 750 °C (c), 800 °C (d), 850 °C (e), 900 °C (f, g) and 950 °C (h, i).

precursors calcined at 450 °C. However, for the sample calcined at 550 °C, better crystallized and smaller particle size morphology can be observed, which were consistent with the results of XRD.

Fig. 4c–i displays the morphologies of the $LiNi_{0.5}Mn_{1.5}O_4$ cathode materials prepared under different calcining temperatures of 750, 800, 850, 900, 950 °C, respectively. With the increase of the calcining temperature, the particle size is increased, and the particle shape became more uniform with clear and smooth surface facets, implying that the samples were well crystallized with the increase of calcining temperature. Fig. 4g and i exhibits high-magnification images of the sample calcined at 900 and 950 °C, it is clearly that the sample prepared at 900 °C possesses full crystal surface and less agglomeration, which is the key factor to the higher electrochemical performance. The average particle size of these powders is around 1.5 μm, meanwhile, the sample calcined at 950 °C exhibits larger particle size and serious aggregation.

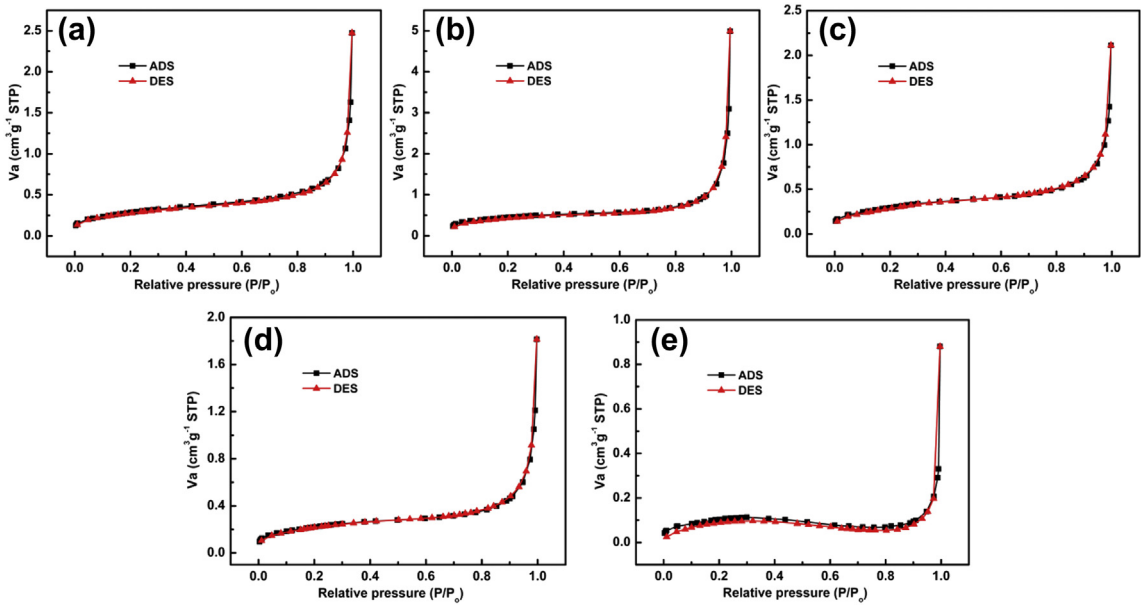

Fig. 5. Adsorption–desorption isotherms of the $LiNi_{0.5}Mn_{1.5}O_4$ samples prepared at different calcining temperatures range from 750 °C (a) to 950 °C (e).

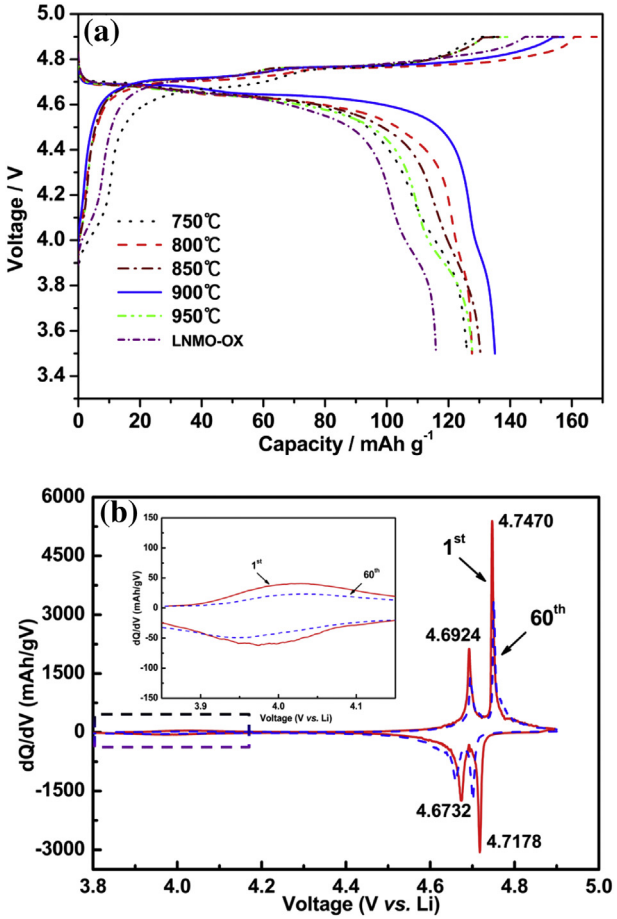

Fig. 6. The charge–discharge curves of the $LiNi_{0.5}Mn_{1.5}O_4$ cathode materials (a), and differential capacity curves, d*Q*/d*V* vs. *V*, of $LiNi_{0.5}Mn_{1.5}O_4$ calcined at 900 °C (b), the values at the peaks are given in voltage in the first cycle.

Fig. 5 exhibits the N_2 adsorption–desorption isotherms of the samples calcined at different temperature, and the specific surface areas calculated from isotherms of the $LiNi_{0.5}Mn_{1.5}O_4$ samples are 1.015, 1.549, 1.053, 0.7282 and 0.3602 $m^2\ g^{-1}$, respectively, for the samples calcined at temperature from 750 to 950 °C.

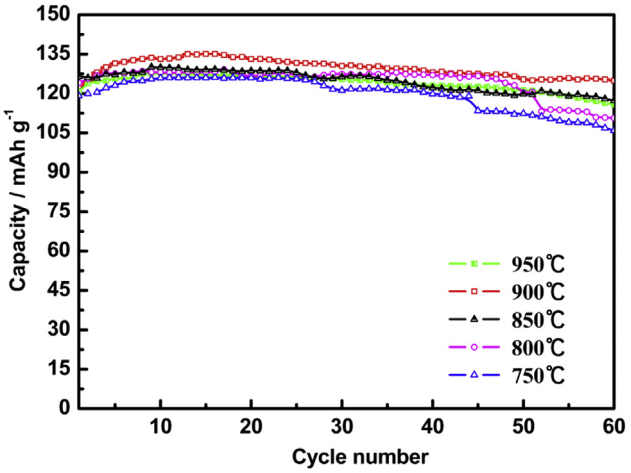

Fig. 7. Discharge capacities vs. cycle number of the $LiNi_{0.5}Mn_{1.5}O_4$ cathode materials.

3.3. Electrochemical characterization

Fig. 6a shows the charge–discharge curves of the $LiNi_{0.5}Mn_{1.5}O_4$ cathode materials at the 10th cycle. The testing cells were subjected to charge and discharge cycling in a voltage range of 3.5–4.9 V under a constant current rate of 0.1C (current density of 14.7 mA g^{-1}). The cell exhibited a long 4.7 V plateau followed by a much shorter 4.0 V plateau; the former could be attributed to the Ni^{4+}/Ni^{2+} redox pair and the latter to the Mn^{4+}/Mn^{3+} redox pair [30]. The discharge capacities of $LiNi_{0.5}Mn_{1.5}O_4$ active materials ranged from 126 to 136 mAh g^{-1}, varying with the calcining temperature, and the material calcined at 900 °C exhibited highest discharge capacity (136 mAh g^{-1}). However, the discharge capacity of the sample LNMO-OX, prepared by mixing and milling Mn–Ni oxalate with lithium salt directly and calcined at 900 °C, is only 115 mAh g^{-1}, indicating that the spinel oxide intermediate plays an important role for the high performance of the final $LiNi_{0.5}Mn_{1.5}O_4$ material.

Generally, the capacity at about 4.0 V plateau can be used to evaluate the relative concentration of Mn^{3+} ions semi-quantificationally, and the contents of Mn^{3+} ions is related to the disorder structure. From the discharge curves, we can see that all of the samples present a small capacity at about 4.0 V plateau, implying that all the samples may mainly have space group of Fd-3m. The sample calcined at 800 °C has the smallest capacity at 4.0 V plateau, indicating the sample obtained under 800 °C may contain

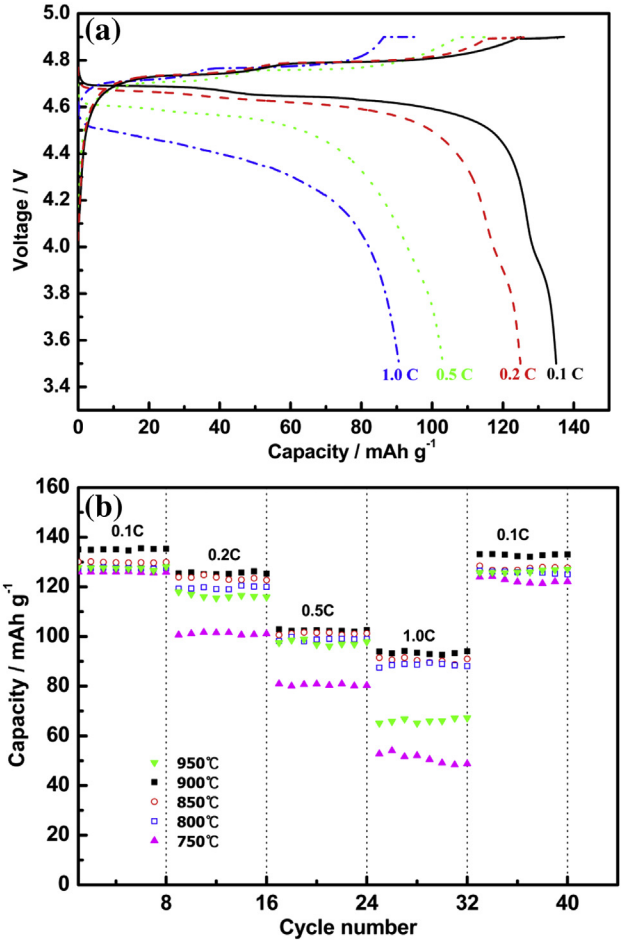

Fig. 8. Discharge curves of the $LiNi_{0.5}Mn_{1.5}O_4$ prepared at 900 °C (a), and capacity retentions of $LiNi_{0.5}Mn_{1.5}O_4$ prepared at different temperatures (b), at various rates: 0.1, 0.2, 0.5, and 1.0C.

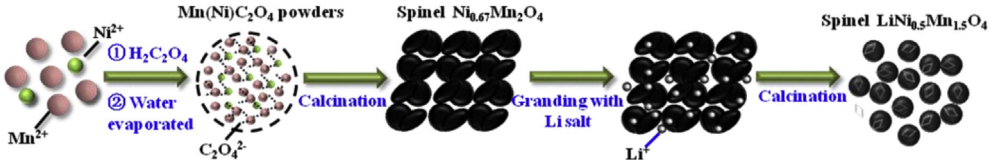

Fig. 9. Schematic illustration of the formation procedure of $LiNi_{0.5}Mn_{1.5}O_4$ materials.

least Mn^{3+} ions and have highest ratio of ordered structure. When the calcining temperature higher than 800 °C, the contents of Mn^{3+} are increased with the increase of calcining temperatures, this result is quite consistent with FTIR data.

To further understand the plateaus of this high voltage material, dQ/dV (Q = specific capacity and V = voltage) profile of the initial and the 60th charge/discharge cycles of the samples prepared at 900 °C was presented in Fig. 6b. The evident voltage plateaus at 4.7470 and 4.7178 V on charge–discharge can be attributed to the Ni^{4+}/Ni^{3+} redox, and the 4.6924 and 4.6732 V plateaus are due to the Ni^{3+}/Ni^{2+} redox, while the remanent peak on dQ/dV profile at about 4.0 V is attributed to the Mn^{4+}/Mn^{3+} redox, which is corresponding to lithium ion insertion into the 8a tetrahedral sites of the cubic spinel structure [31]. With the cycle number increased, the intensity of the peaks decreased and the gap between two redox potential increased. From the increased gap between the redox potential, it can be suggested that the Li ions require more energy to intercalate/deintercalate into/from the host structure, which is resulted from larger polarization of the materials [32].

Fig. 7 presents the cycle performance of the $LiNi_{0.5}Mn_{1.5}O_4$ cathode materials between 3.5 and 4.9 V at the same specific discharge current of 14.7 mA g^{-1} (0.1C rate). It is clearly that the material calcined at 900 °C exhibits the highest discharge capacity and the best cycle stability, the capacity retention is high up to 93% after 50 cycles.

Fig. 8a shows the voltage profiles of $LiNi_{0.5}Mn_{1.5}O_4$ materials calcined at 900 °C at various rates. With the increase of discharge rate, the discharge voltage plateau was decreased gradually. It should be pointed out that the decrease rate of the voltage plateau is a little bit higher than the results reported previously by other groups [33], it may be caused by the larger impedance of the test cells, probably resulting from the separator.

Fig. 8b compares the capacity retentions of samples at various discharge rates. It can be seen that all the five samples exhibit rather reproducible capacities during 8 cycles test at each current rate and the capacity can be retrieved when the 0.1C rate is applied again. This result confirms that this synthesis method is reliable to prepare stable $LiNi_{0.5}Mn_{1.5}O_4$ materials. Furthermore, it is clear that the $LiNi_{0.5}Mn_{1.5}O_4$ materials prepared at 900 °C not only shows the highest capacities, but also best performance at high discharge rate. Once the rate changed from 0.1C to 1C, the performance decrease of the sample calcined at 900 °C is 29.2%, but for the sample calcined at 750 °C, the decrease is high up to 44.8%.

3.4. Mechanism for the formation of the materials

Based on above investigation, we suggested the possible formation mechanism of the spinel $LiNi_{0.5}Mn_{1.5}O_4$. As shown in Fig. 9, in the first co-precipitation stage, we firstly prepared an oxalate co-precipitate of nickel and manganese, then a spinel oxides precursor was obtained through calcining the oxalate powders at an appropriate temperature. Due to that the oxide is derived from oxalate, it resulted in good morphology, higher surface area, and better structure. In the second step, the Li ions were embedded into the lattice of spinel oxides precursor by calcining the mixture of $Ni_{0.67}Mn_2O_4$ with Li_2CO_3, the mixture was ball milled with the alcohol as the dispersing agent prior to the calcination. In this process, the spinel $LiNi_{0.5}Mn_{1.5}O_4$ materials formed based on the transition spinel oxides. It should be pointed out that high-purity $LiNi_{0.5}Mn_{1.5}O_4$ cathode material is easily acquired by this two-step approach, maybe the spinel oxide precursor plays an important role for the formation of high purity and high performance materials.

4. Conclusion

In summary, $LiNi_{0.5}Mn_{1.5}O_4$ cathode materials were successfully synthesized through a two-step approach. The calcining temperature yielded a pronounced effect on the crystalline structure, morphologies and electrochemical properties of the materials. The materials exhibited excellent performance, high capacity and good cyclic stability. We suggested that the high performance of the materials may be strongly related to the spinel oxide precursor, due to the oxide precursor is derived from oxalate.

Acknowledgments

This work was financially supported by the National Scientific Foundation of China (NSFC Project nos. 21076089, 20876062, 20673040), and Doctoral Fund of Ministry of Education of China (20110172110012).

References

[1] O.K. Park, Y. Cho, S. Lee, H.C. Yoo, H.K. Song, J. Cho, Energy Environ. Sci. 4 (2011) 1621–1633.
[2] M.S. Whittingham, Chem. Rev. 104 (2004) 4271–4302.
[3] D. Aurbach, M.D. Levi, K. Gamulski, B. Markovsky, G. Salitra, E. Levi, U. Heider, L. Heider, R. Oesten, J. Power Sources 81–82 (1999) 472–479.
[4] H.W. Lee, P. Muralidharan, R. Ruffo, C.M. Mari, Y. Cui, D.K. Kim, Nano Lett. 10 (2010) 3852–3856.
[5] A. Kraytsberg, Y. Ein-Eli, Adv. Energy Mater. 2 (2012) 922–939.
[6] R. Santhanam, B. Rambabu, J. Power Sources 195 (2010) 5442–5451.
[7] R. Marom, S.F. Amalraj, N. Leifer, D. Jacob, D. Aurbach, J. Mater. Chem. 21 (2011) 9938–9954.
[8] Z. Zhu, H. Yan, D. Zhang, W. Li, Q. Lu, J. Power Sources 224 (2013) 13–19.
[9] X. Ma, B. Kang, G. Ceder, J. Electrochem. Soc. 157 (2010) A925–A931.
[10] N.M. Hagh, G.G. Amatucci, J. Power Sources 195 (2010) 5005–5012.
[11] X. Zhang, F. Cheng, K. Zhang, Y. Liang, S. Yang, J. Liang, J. Chen, RSC Adv. 2 (2012) 5669–5675.
[12] Z. Zhu, D. Zhang, H. Yan, W. Li, Qilu, J. Mater. Chem. A 1 (2013) 5492–5496.
[13] G.Q. Liu, Y.J. Wang, Qilu, W. Li, Chenhui, Electrochim. Acta 50 (2005) 1965–1968.
[14] J. Cabana, M. Casas-Cabanas, F.O. Omenya, N.A. Chernova, D. Zeng, M.S. Whittingham, C.P. Grey, Chem. Mater. 24 (2012) 2952–2964.
[15] D. Liu, J. Han, J.B. Goodenough, J. Power Sources 195 (2010) 2918–2923.
[16] Y. Sun, Y. Yang, X. Zhao, H. Shao, Electrochim. Acta 56 (2011) 5934–5939.
[17] D. Li, A. Ito, K. Kobayakawa, H. Noguchi, Y. Sato, J. Power Sources 161 (2006) 1241–1246.
[18] K. Hoshina, K. Yoshima, M. Kotobuki, K. Kanamura, Solid State Ionics 209–210 (2012) 30–35.
[19] H. Duncan, Y. Abu-Lebdeh, I.J. Davidson, J. Electrochem. Soc. 157 (2010) A528–A535.
[20] E.-S. Lee, K.-W. Nam, E. Hu, A. Manthiram, Chem. Mater. 24 (2012) 3610–3620.
[21] J. Song, D.W. Shin, Y. Lu, C.D. Amos, A. Manthiram, J.B. Goodenough, Chem. Mater. 24 (2012) 3101–3109.
[22] J. Cabana, H. Zheng, A.K. Shukla, C. Kim, V.S. Battaglia, M. Kunduraci, J. Electrochem. Soc. 158 (2011) A997–A1004.

[23] B. Gillot, J. Baudour, F. Bouree, R. Metz, R. Legros, A. Rousset, Solid State Ionics 58 (1992) 155–161.
[24] J.C. Arrebola, A. Caballero, L. Hernán, J. Morales, Eur. J. Inorg. Chem. 2008 (2008) 3295–3302.
[25] L. Wang, H. Li, X. Huang, E. Baudrin, Solid State Ionics 193 (2011) 32–38.
[26] J.H. Kim, S.T. Myung, C. Yoon, S. Kang, Y.K. Sun, Chem. Mater. 16 (2004) 906–914.
[27] R. Alcantara, M. Jaraba, P. Lavela, J. Tirado, E. Zhecheva, R. Stoyanova, Chem. Mater. 16 (2004) 1573–1579.
[28] M. Kunduraci, J.F. Al-Sharab, G.G. Amatucci, Chem. Mater. 18 (2006) 3585–3592.
[29] D.W. Shin, C.A. Bridges, A. Huq, M.P. Paranthaman, A. Manthiram, Chem. Mater. 24 (2012) 3720–3731.
[30] M. Kunduraci, G.G. Amatucci, J. Electrochem. Soc. 153 (2006) A1345–A1352.
[31] M. Kunduraci, G.G. Amatucci, J. Power Sources 165 (2007) 359–367.
[32] J.H. Kim, N.P.W. Pieczonka, Z.C. Li, Y. Wu, S. Harris, B.R. Powell, Electrochim. Acta 90 (2013) 556–562.
[33] L. Zhou, D. Zhao, X. Lou, Angew. Chem. Int. Ed. 51 (2012) 239–241.